

# Plasma Clearance Kinetics of the Amyloid-related High Density Lipoprotein Apoprotein, Serum Amyloid Protein (ApoSAA), in the Mouse

## EVIDENCE FOR RAPID ApoSAA CLEARANCE

JEFFREY S. HOFFMAN and EARL P. BENDITT, *Department of Pathology, University of Washington, Seattle, Washington 98195*

**ABSTRACT** The plasma clearance kinetics of the amyloid-related high density lipoprotein (HDL) apoprotein serum amyloid protein (apoSAA) was examined in BALB/c mice by two different methods, using labeled  $^{125}\text{I}$ -apoSAA-rich HDL and unlabeled plasma apoSAA (clearance monitored by radioimmunoassay). The plasma half-life of apoSAA, estimated by both methods, was on the order of 75–80 min, as compared with a value of  $\sim 11$  h for mouse apoA-I. In trace-labeling studies, the rapid plasma clearance of both major  $^{125}\text{I}$ -labeled apoSAA isotypes was observed; this metabolic behavior was unique to these polypeptides among HDL apoproteins. The property of rapid plasma clearance was lost upon purification and reconstitution of  $^{125}\text{I}$ -apoSAA with HDL, indicating that this property is labile to denaturing conditions. Studies aimed at determining the metabolic fate of  $^{125}\text{I}$ -apoSAA gave no evidence for either the selective excretion of  $^{125}\text{I}$ -apoSAA or clearance to unique tissue sites as compared with other  $^{125}\text{I}$ -HDL apoproteins.

## INTRODUCTION

The serum amyloid protein (12-kD apoSAA)<sup>1</sup> is a high density lipoprotein (HDL) apoprotein (1–3) having  $\text{NH}_2$ -terminal amino acid sequence homology with the major polypeptide constituent (8.5 kD amyloid protein AA) of lesions present in a common form of amyloidosis (4). It is now well established that apoSAA is an acute-phase plasma protein, exhibiting dramatic ele-

variations in plasma concentration in response to a variety of disease processes and pathologic conditions (5). Hepatic synthesis of apoSAA (6, 7) is stimulated indirectly by the potent apoSAA inducer, bacterial endotoxin, via a monocyte cell product (7), possibly interleukin I (8). Chronic elevations in serum apoSAA levels, associated with long-standing inflammation and infection (9), are predisposing to amyloidosis in which a likely apoSAA fragment (amyloid protein AA) forms fibrillar deposits found in a variety of tissues (10).

Little is known about the function of apoSAA and apoSAA-rich HDL in the host response to injury. Similarly obscure is the putative mechanism by which the altered metabolism of apoSAA leads to the formation of protein AA deposits during amyloidogenesis. To gain insight into these processes, we began studies of the metabolism of apoSAA, using a convenient and extensively studied species in amyloidosis research, the mouse. We recently presented evidence that murine apoSAA is secreted in monomeric form (11) and is associated with a subset of plasma HDL during the acute-phase response (12). In this report we describe the results of turnover studies in which we compared the plasma clearance kinetics of mouse apoSAA with that of other mouse HDL apoproteins.

## METHODS

**Analytical procedures.** ApoSAA concentrations were estimated by radioimmunoassay (RIA) as described in detail elsewhere (12), using a rabbit antiserum prepared against the (8.5 kD) mouse amyloid protein AA, the immunoreactive  $\text{NH}_2$ -terminal homologue of serum apoSAA (13). Samples were preheated at  $60^\circ\text{C}$  for 1 h to maximize immunoreactivity of apoSAA (1).

Total protein was estimated colorimetrically using bovine serum albumin as standard (14).

**Stimulation of mice and blood collection.** 6–8-wk-old

*Received for publication 2 November 1981 and in revised form 15 December 1982.*

<sup>1</sup> *Abbreviations used in this paper:* apoA-I, apolipoprotein A-I; apoSAA, serum amyloid protein; SDS-PAGE, sodium dodecyl sulfate-polyacrylamide gel electrophoresis.

BALB/c mice were used throughout; mice were fed ad lib. Mice used to prepare plasma or apoSAA-rich HDL for clearance studies were injected intraperitoneally with bacterial endotoxin (50  $\mu$ g lipopolysaccharide W from *Salmonella typhi*, Difco Laboratories, Detroit, MI), a procedure which routinely elevates apoSAA levels at least 50-fold that of basal levels ( $4 \pm 1$   $\mu$ g/ml), to 250–300  $\mu$ g apoSAA/ml plasma at 20 h postinjection (12). Blood (0.5–1.0 ml/mouse) was collected by cardiac puncture of ether-anesthetized mice. HDL was prepared from serum; for experiments using plasma, blood was collected in heparinized tubes.

**Preparation and labeling of HDL.** Whole HDL (1.063 <  $d$  < 1.21 g/ml) was prepared by sequential ultracentrifugation (12). The solution densities were adjusted to 1.063 g/ml and 1.21 g/ml by addition of solid KBr and solutions containing KBr, 0.01% Na<sub>2</sub>EDTA, and 0.05% NaN<sub>3</sub>. Preparative ultracentrifugation was performed in 6.4 ml capacity polyallomer tubes in a Beckman 50.3 Ti rotor (Beckman Instruments, Inc., Spinco Div., Palo Alto, CA) at 50,000 rpm for 18 h at 10°C. Uppermost (1.5 ml) fractions were collected by careful aspiration.

Labeling with <sup>125</sup>I (carrier-free Na-<sup>125</sup>I, 15–17 Ci/mM; Amersham Corp., Arlington Heights, IL) was performed using the ICL method (15) as modified by Bilheimer et al. (16). The reaction was performed at a molar I/protein ratio of <1, assuming an average protein content of 125,000 g/mol HDL. Specific activities ranging from 3 to  $10 \times 10^5$  cpm/ $\mu$ g protein were obtained at labeling efficiencies ranging from 10 to 40%. Unbound iodine was removed by dialysis in Spectrapor 3 tubing (Spectrum Medical Industries Inc., Los Angeles, CA), against 0.85% NaCl, 0.01 M NaH<sub>2</sub>PO<sub>4</sub>, 0.01% Na<sub>2</sub>EDTA, and 3 mM KI, pH 7.4 until the ratio of trichloroacetic acid (TCA)-precipitable to total counts was >0.97. Labeled lipids, measured by extraction at –10°C with 3:2 ethanol/diethyl ether (17), comprised <10% of the total lipoprotein-bound counts. The <sup>125</sup>I-labeled, dialyzed HDL was again centrifuged at  $d = 1.21$  g/ml to remove contaminating or delipidated protein. Greater than 80% of the applied radioactivity was recovered in the upper quarter of the tube following this spin; >90% of the radioactivity recovered in bottom fractions was associated with albumin and non-HDL associated protein, as judged by sodium dodecyl sulfate (SDS) gel electrophoresis and autoradiography. The ultracentrifugally washed <sup>125</sup>I-HDL preparation was dialyzed against 0.85% NaCl, 0.01 M NaH<sub>2</sub>PO<sub>4</sub>, pH 7.4 (PBS), before intravenous administration to mice.

**Clearance of <sup>125</sup>I-labeled HDL.** 6–8-wk-old BALB/c mice were injected via the tail vein with 0.1–0.3 ml of <sup>125</sup>I-HDL. Mice were periodically ether-anesthetized and bled (50  $\mu$ l) into heparinized capillary tubes by sampling of the retroorbital venous plexus. Small but significant dilution effects accompanying repeated bleedings were minimized by rotational sampling such that no mouse was bled more than four times in the course of an experiment. Pooled plasma samples recovered at various time intervals were spun in 6.5-ml capacity tubes for 18 h at 50,000 rpm and 10°C in a Beckman 50.3 Ti rotor, following adjustment of the solution density to 1.21 g/ml. Greater than 90% of the plasma radioactivity was recovered in uppermost (1.5 ml) tube fractions, which were dialyzed in Spectrapor 3 tubing (Spectrum Scientific Corp., Newark, DE) against 0.5% acetic acid and lyophilized. The lyophilized samples were solubilized in SDS sample buffer and aliquots electrophoresed in 11.5% polyacrylamide (18). Approximately 10  $\mu$ g of unlabeled apoSAA-rich HDL apoproteins were added per lane, for the purpose of staining and visualization of protein bands.

Clearance rates of <sup>125</sup>I-HDL apoproteins were estimated

as follows: bands were excised from stained, dried gels, and counted. The percentage of total gel-bound radioactivity measured in individual protein bands, multiplied by the plasma concentration of radioactivity at various sampling times, generated a set of points from which plasma clearance curves for individual apoproteins were obtained.

In experiments in which urinary output of radioactivity was measured, samples were taken from bladder contents of mice killed at various time intervals. For tissue localization studies, ether-anesthetized mice were perfused via the left ventricle with ~15 ml of PBS followed by 20 ml of 2% glutaraldehyde, 1% paraformaldehyde, 0.1 M NaH<sub>2</sub>PO<sub>4</sub>, pH 7.4, at a rate of ~10 ml/min, and the perfusate drained via the inferior vena cava.

**Urea-SDS-polyacrylamide gel electrophoresis (PAGE).** Urea-SDS-PAGE was performed in 10 cm  $\times$  12.5 cm  $\times$  0.75-mm slab gels containing 11.5% polyacrylamide (Eastman Kodak Co., Rochester, NY). The resolving gel was prepared as described by Goldsmith et al. (18); the stacking gel, running buffer, and sample buffer were prepared according to Laemmli (19). Samples were electrophoresed at 22 mA (constant) until the tracking dye reached the bottom of the gel. Gels were fixed in 2% glutaraldehyde, 50% methanol, and 10% acetic acid for 1 h, then stained in 0.05% Coomassie blue G-250, 25% isopropyl alcohol, 10% acetic acid, and destained in 10% acetic acid. The gels were then dried and autoradiographed with Kodak XAR-5 film (Eastman Kodak Co.) at –70°C using a DuPont Cronex Hi-Plus intensifying screen (E. I. DuPont de Nemours and Co., Wilmington, DE). Exposure times of 24–48 h were necessary for gels containing 10,000–20,000 cpm/lane.

**Isoelectric focusing and reconstitution of purified <sup>125</sup>I-apoproteins.** Isoelectric focusing of delipidated (17) <sup>125</sup>I-apoSAA-rich HDL ( $3\text{--}10 \times 10^5$  cpm/ $\mu$ g protein) was performed in 3  $\times$  12.5-cm cylindrical polyacrylamide gels as described by Gidez et al. (20, 12), using pH 3.5–10 ampholytes (LKB Instruments Inc., Rockville, MD). ApoA-I and apoSAA-containing bands were located by reference to fixed, stained companion gels, and were excised, diced into small pieces, and suspended in ~20 vol of 6 M guanidine/HCl. Apoproteins were eluted by overnight incubation at 5°C with low-speed vortexing, and guanidine removed by dialysis against PBS in Spectrapor 3 tubing. The dialyzed <sup>125</sup>I-apoprotein solutions were each incubated for 1 h at 37°C with 1 ml apoSAA-rich serum, prepared from endotoxin-treated mice as described above. Resulting <sup>125</sup>I-apoprotein/HDL complexes were isolated by ultracentrifugation as described above, at densities of 1.063 and 1.21 g/ml. Incorporation of 35–40% of the <sup>125</sup>I-labeled apoprotein into the HDL was achieved by this method. Following dialysis against PBS, this material was administered to mice.

## RESULTS

SDS-PAGE patterns of normal (control) mouse HDL (1.063 <  $d$  < 1.21 g/ml) and HDL from serum obtained 20 h after endotoxin administration (50  $\mu$ g *S. typhi* lipopolysaccharide, i.p.) are shown in Fig. 1 (a, b). A major (28 kD) polypeptide, apolipoprotein A-I (apoA-I), and several smaller molecular mass (6–10 kD) apoproteins are the principal constituents of control mouse HDL. HDL from endotoxin-treated mice contain, in addition, two mouse apoSAA isotypes (12.6-kD apoSAA<sub>1</sub> and 11.8-kD apoSAA<sub>2</sub>), constituting ~20–25% of the total HDL protein content (12).

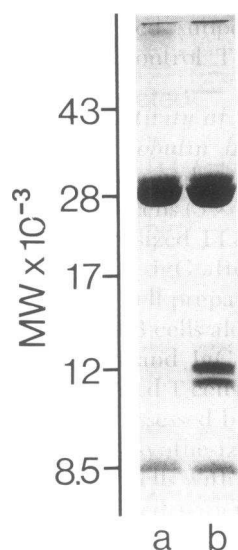


FIGURE 1 SDS-PAGE of (a) normal mouse HDL, and (b) HDL from mouse plasma obtained 20 h after intraperitoneal administration of (50  $\mu$ g) bacterial endotoxin. An 11.5% polyacrylamide resolving gel containing 6.4 M urea was used (17). Approximately 10  $\mu$ g loaded/lane; molecular weight markers were ovalbumin (43,000-mol wt), human apoA-I (28,000-mol wt), horse heart myoglobin (17,000-mol wt), cytochrome *c* (12,000-mol wt), and monkey amyloid protein AA (8,500-mol wt).

The metabolism of  $^{125}$ I-control HDL and  $^{125}$ I-apoSAA-rich HDL was studied by intravenous administration of the respective  $^{125}$ I-labeled whole HDL preparations into two groups of mice, and the plasma clearance of radioactivity was monitored by periodic blood sampling. A comparison of the plasma clearance curves generated with  $^{125}$ I-control HDL and  $^{125}$ I-apoSAA-rich HDL indicates that these preparations are metabolically distinct (Fig. 2). Both curves exhibited an early, rapidly clearing component between 0 and 6 h followed by a log-linear component between 6 and 48 h postinjection (points beyond 24 h not shown). Half-life estimates from the slopes of terminal components (6–48 h) of these curves are not significantly different:  $13.9 \pm 2.8$  (mean  $\pm$  SD,  $n = 6$  experiments) for  $^{125}$ I-apoSAA-rich HDL and  $15.1 \pm 1.4$  (mean  $\pm$  SD,  $n = 3$  experiments) for  $^{125}$ I-control HDL, values similar to that reported for the closely related species, rat (21, 22). These curves do not, however, overlap, since a greater proportion of  $^{125}$ I-apoSAA-rich HDL was cleared from the plasma between 0 and 6 h as compared with  $^{125}$ I-control HDL. The rapidly clearing component constituted 50% ( $49 \pm 7$ ,  $n = 4$  experiments) of the administered  $^{125}$ I-apoSAA-rich HDL as compared with a value of  $\sim 25\%$  ( $24 \pm 6$ ,  $n = 3$  experiments) for  $^{125}$ I-control HDL, as estimated by extrapolation of the log-linear portions (6–24 h) of these

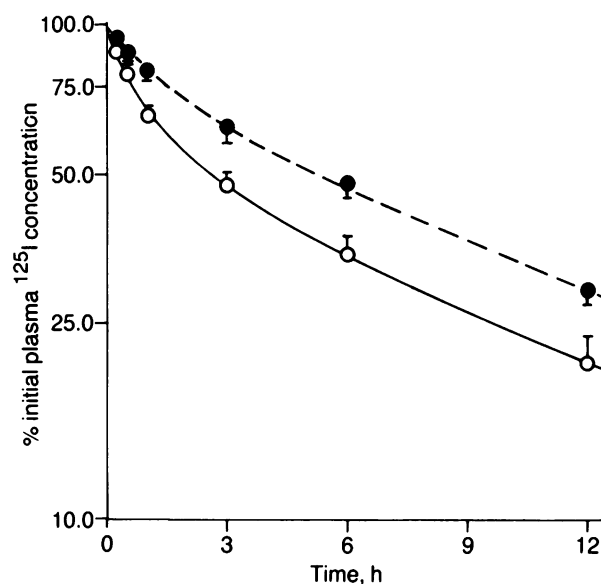


FIGURE 2 Plasma clearance rates of  $^{125}$ I-control HDL (●) and  $^{125}$ I-apoSAA-rich HDL (○) in mice following intravenous administration. Results are plotted as percentage of the initial (5-min postinjection) plasma radioactivity concentration. Points and bars represent means  $\pm$  SD of samples from three mice.

curves to  $t = 0$ . The divergence of these curves was statistically significant ( $P < 0.01$ ) for paired data points at all time intervals sampled beyond 30 min postinjection.

These differences might be accounted for by the rapid plasma clearance of one or more components present in  $^{125}$ I-apoSAA-rich HDL but absent in  $^{125}$ I-control HDL, or might alternatively be a property generally shared by all apoproteins in  $^{125}$ I-apoSAA-rich HDL. To further examine these possibilities, the plasma clearance kinetics of individual  $^{125}$ I-apoproteins in  $^{125}$ I-apoSAA-rich HDL were examined by SDS/PAGE of lipoproteins ( $d < 1.21$  g/ml) recovered from pooled plasma samples obtained at various time intervals following intravenous administration of  $^{125}$ I-apoSAA-rich HDL. The percent distribution of total radioactivity incorporated into apoA-I, apoSAA, and small molecular mass (6–10 kDa) apoproteins was  $23 \pm 2$ ,  $24 \pm 3$ , and  $42 \pm 4\%$ , respectively (means  $\pm$  SD,  $n = 3$  samples) for  $^{125}$ I-apoSAA-rich HDL. After intravenous administration of  $^{125}$ I-apoSAA-rich HDL a rapid and specific depletion of both  $^{125}$ I-apoSAA isotypes from the pool of circulating  $^{125}$ I-HDL apoproteins was observed (Fig. 3). By 6–12 h postinjection, no autoradiographic bands corresponding to apoSAA isotypes were apparent.

Examination of the plasma clearance kinetics of individual  $^{125}$ I-apoproteins (Fig. 4) reveals dramatic differences in that of apoSAA as compared with other

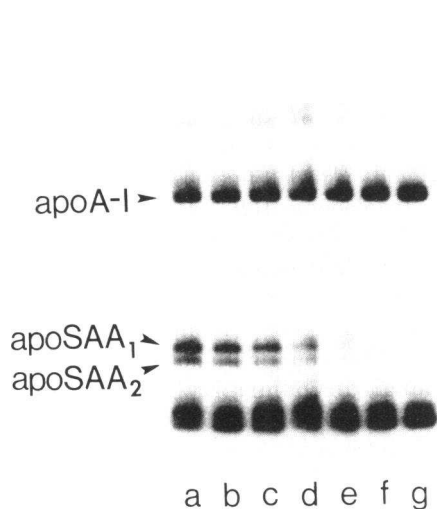


FIGURE 3 Autoradiogram of  $^{125}\text{I}$ -apoproteins recovered from mouse plasma after intravenous administration of  $^{125}\text{I}$ -apoSAA-rich HDL. Apoproteins recovered from plasma samples at (a) 5 min; (b) 15 min; (c) 30 min; (d) 1 h; (e) 3 h; (f) 6 h; and (g) 12 h after intravenous administration of  $^{125}\text{I}$ -apoSAA-rich HDL were autoradiographed following SDS-polyacrylamide (11.5%) slab gel electrophoresis (Methods). Approximately 10,000 cpm loaded per lane.

HDL apoproteins. The curve generated for apoA-I was biphasic with  $\sim 45\%$  of the  $^{125}\text{I}$ -apoA-I cleared during the first 3 h, the bulk of the remaining labeled species exhibiting log-linear kinetics with a plasma half-life of  $\sim 11$  h. Although the smaller molecular mass (6–10 kD) apoproteins were not sufficiently resolved in the gel system used to permit their individual examination, a similar curve to that generated with  $^{125}\text{I}$ -apoA-I was obtained for the total population of  $^{125}\text{I}$ -apoproteins in this size range. In contrast, the curve generated for  $^{125}\text{I}$ -apoSAA indicated rapid plasma clearance, with the majority of the  $^{125}\text{I}$ -apoSAA lost from the plasma by 6 h. Flattening out of this curve to a log-linear form did not take place within the first 12 h after the administration of  $^{125}\text{I}$ -apoSAA-rich HDL, although  $<2\%$  of the original plasma activity found in gel slices containing  $^{125}\text{I}$ -apoSAA remained at this time. Close examination of grossly overexposed autoradiograms indicated that the small amount of residual radioactivity present in this region of the gel at 12 h was largely associated with a polypeptide of slightly lower electrophoretic mobility than  $^{125}\text{I}$ -apoSAA<sub>1</sub>, rather than a subpopulation of slower-clearing  $^{125}\text{I}$ -apoSAA. The close proximity of this “contaminating” band to apoSAA<sub>1</sub> did not allow their separation by densitometric methods; therefore, measurements of radioactivity in gel slices at 12 h (and beyond) did not accurately reflect  $^{125}\text{I}$ -apoSAA content per se. A provisional estimate of the  $^{125}\text{I}$ -apoSAA clearance rate by linear regression analysis of points obtained at 0–6 h

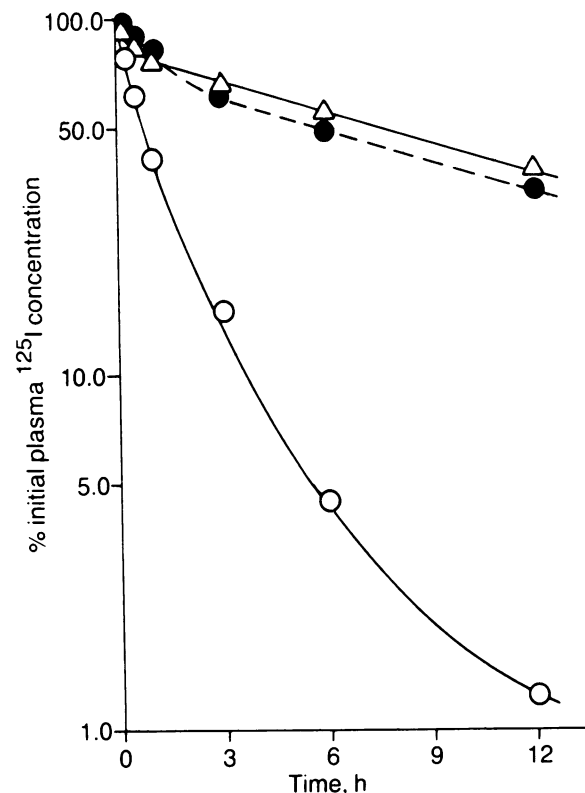


FIGURE 4 Plasma clearance rates of  $^{125}\text{I}$ -labeled apoproteins following intravenous administration of  $^{125}\text{I}$ -apoSAA-rich HDL. Clearance rates of  $^{125}\text{I}$ -apoA-I ( $\Delta$ ),  $^{125}\text{I}$ -apoSAA ( $\circ$ ), and  $^{125}\text{I}$ -(small-molecular weight HDL apoproteins) ( $\bullet$ ) were estimated (Methods). Points represent mean values for three experiments.

was  $\sim 85$  min;  $\sim 95\%$  of the applied dose was cleared during this interval.

One possible route of rapid  $^{125}\text{I}$ -apoSAA clearance, via urinary excretion, was examined. Urine samples taken at 0.5, 1, 3, 6, and 12 h after administration of  $^{125}\text{I}$ -apoSAA-rich HDL were tested for the presence of TCA (10% wt/vol)-precipitable polypeptides. At all time intervals tested,  $>99\%$  of the urine radioactivity was TCA-soluble; furthermore, no TCA-soluble  $^{125}\text{I}$ -apoSAA polypeptides were detected by immunoprecipitation with antiserum prepared against mouse amyloid protein AA. In another experiment in which mice were confined in metabolic cages,  $\sim 70 \pm 9\%$  ( $n = 3$ ) of the radioactivity lost from the plasma during the first 12 h following administration of  $^{125}\text{I}$ -apoSAA-rich HDL was recovered in urine and feces. These results show that although the bulk of the plasma radioactivity was excreted, there was no evidence indicating the selective urinary loss of  $^{125}\text{I}$ -apoSAA or  $^{125}\text{I}$ -apoSAA fragments.

A possible explanation for the rapid plasma clearance of  $^{125}\text{I}$ -apoSAA observed in the experiments de-

scribed above is that apoSAA is uniquely susceptible among HDL apoproteins to labeling artifact. Alternatively, rapid plasma clearance might be due to the susceptibility of apoSAA to denaturing conditions involved in the preparation of HDL (e.g., high salt concentrations and prolonged ultracentrifugation). Experiments aimed at addressing these possibilities were performed, in which freshly isolated plasma, highly enriched in apoSAA, was administered to normal mice and apoSAA clearance monitored by RIA. 200–300  $\mu$ l of donor plasma, containing  $>300 \mu\text{g}$  apoSAA/ml was collected and immediately (within 3 h) injected intravenously into normal syngeneic mice, a procedure that elevates apoSAA levels  $>20$ -fold in recipients. The plasma clearance of apoSAA in recipient mice, monitored by RIA, exhibited monoexponential kinetics through 3 h postinjection, with a plasma half-life of  $\sim 72$  min (Fig. 5). These experiments clearly indicate that rapid plasma clearance of apoSAA observed in trace-labeling experiments does not result from labeling or preparative artifact but is instead a property of freshly obtained, unpurified, and unlabeled apoSAA.

The unique metabolic behavior of apoSAA observed in the experiments described above led us to inquire about the tissue sites to which apoSAA is cleared and whether these sites are similar to those observed for other HDL apoproteins. To study the metabolic fate of individual apoproteins, we initially used a modification of the method originally described by Shepherd et al. (23) to study apoprotein turnover, in which whole

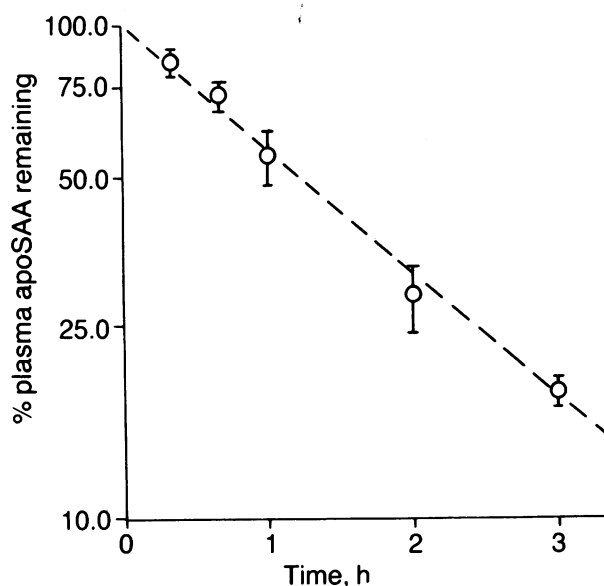


FIGURE 5 Plasma clearance of apoSAA after intravenous administration of apoSAA-rich plasma. Points and bars represent means  $\pm$  SEM for four samples, following subtraction of control (saline-administered) values.

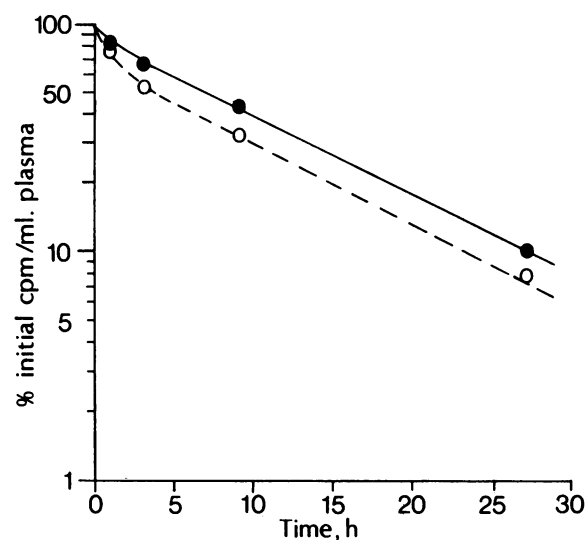


FIGURE 6 Plasma clearance rates of HDL-reconstituted  $^{125}\text{I}$ -apoproteins. Purified  $^{125}\text{I}$ -apoA-I ( $\bullet$ ) and  $^{125}\text{I}$ -apoSAA ( $\circ$ ) were reconstituted with whole (unlabeled) apoSAA-rich HDL and administered intravenously to mice. Points represent mean values for three samples.

(unlabeled) HDL is reconstituted with purified  $^{125}\text{I}$ -apoproteins and administered intravenously. In these experiments we compared the metabolic behavior of HDL-reconstituted  $^{125}\text{I}$ -apoA-I and  $^{125}\text{I}$ -apoSAA. In contrast to those obtained using  $^{125}\text{I}$ -apoSAA-rich HDL, the plasma clearance curves generated using HDL-reconstituted  $^{125}\text{I}$ -apoSAA and  $^{125}\text{I}$ -apoA-I ran in parallel, indicating plasma half-lives of  $\sim 9.7$  and  $10.5$  h, respectively (Fig. 6). The plasma half-life of reconstituted  $^{125}\text{I}$ -apoA-I approximated that measured for  $^{125}\text{I}$ -apoA-I using  $^{125}\text{I}$ -apoSAA-rich HDL (11 h), whereas the bulk of the reconstituted  $^{125}\text{I}$ -apoSAA was cleared more slowly as compared with that obtained using  $^{125}\text{I}$ -apoSAA-rich HDL (85 min). These results indicate that purification and reconstitution minimally affect the clearance rate of  $^{125}\text{I}$ -apoA-I relative to that measured with  $^{125}\text{I}$ -HDL, but dramatically retard the plasma clearance of  $^{125}\text{I}$ -apoSAA. It is also noteworthy that the clearance rates of  $^{125}\text{I}$ -apoA-I and  $^{125}\text{I}$ -apoSAA measured in reconstitution experiments are similar, suggesting a common metabolic pathway for the HDL-reconstituted  $^{125}\text{I}$ -apoproteins.

Since purified, HDL-reconstituted  $^{125}\text{I}$ -apoSAA did not exhibit a similar clearance rate when compared with either that of native (unlabeled) apoSAA or  $^{125}\text{I}$ -apoSAA in  $^{125}\text{I}$ -apoSAA-rich HDL, an alternative approach to studying the metabolic fate of apoSAA was used. Our previous experiments had indicated that  $^{125}\text{I}$ -apoSAA accounted for  $\sim 50\%$  of the cleared radioactivity during the 1st h (estimated from the raw data, Fig. 4) but was of negligible contribution for intervals

beyond 12 h (assuming a plasma half-life of 85 min). We therefore compared the tissue distribution of  $^{125}\text{I}$  during the period of rapid clearance (1 h), during the log-linear clearance phase (24 h), and at the transition between these periods (6 h), following intravenous administration of  $^{125}\text{I}$ -apoSAA-rich HDL. Approximately 9, 6, and 2% of the administered  $^{125}\text{I}$  dose was localized in the major organs studied at 1, 6, and 24 h, respec-

tively. The tissue distribution of label was similar at all time intervals studied (Fig. 7) and comparable to that reported for rat HDL (21, 22), with liver, and to a lesser extent intestines, being major organs of  $^{125}\text{I}$ -apoprotein uptake. We observed no difference in the organ distribution of radioactivity at 1, 6, and 24 h; thus, although  $\sim 95\%$  of the administered apoSAA in  $^{125}\text{I}$ -apoSAA-rich HDL is cleared from the plasma

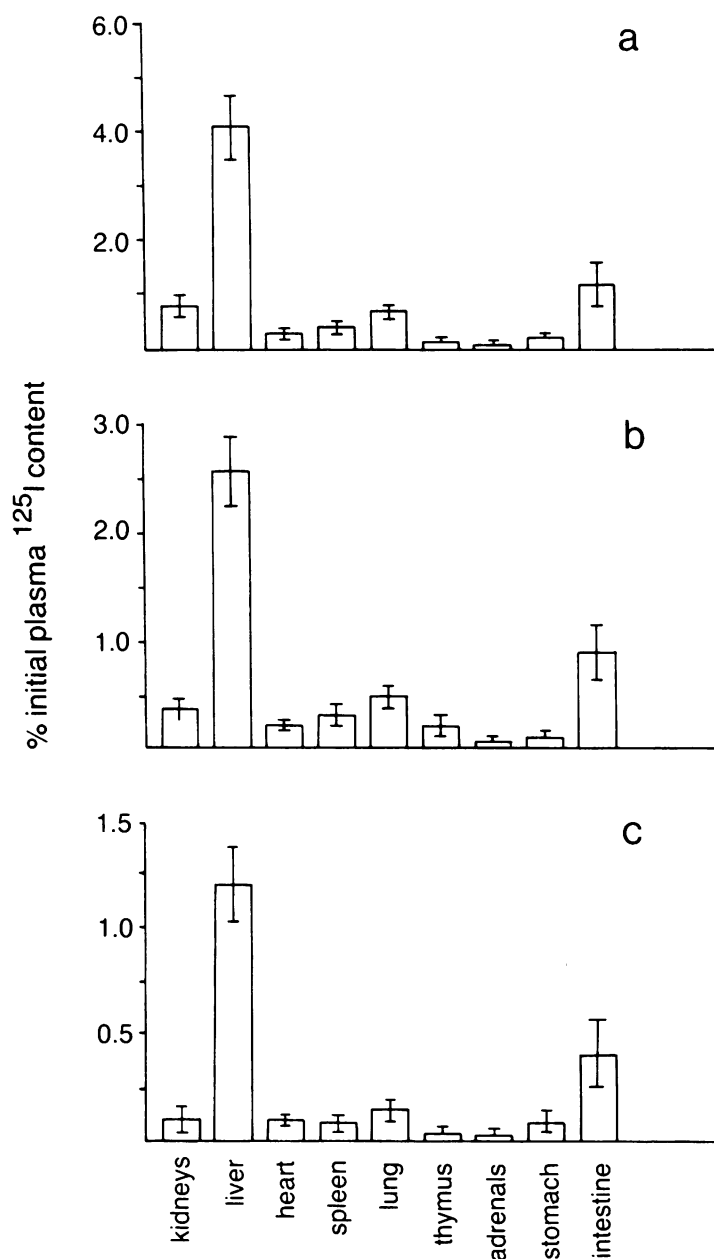


FIGURE 7 Tissue distribution of  $^{125}\text{I}$  after intravenous administration of  $^{125}\text{I}$ -apoSAA-rich HDL. Samples taken at (a) 1 h; (b) 6 h; and (c) 12 h postinjection. Bars represent means  $\pm$  SD of three samples.

within 6 h, we found no evidence that the metabolic fate of label cleared within this time frame (1, 6 h) differed from that cleared later (24 h).

## DISCUSSION

The observation that apoSAA is associated with HDL (1-3) has led us to examine the structural and metabolic aspects of this relationship in detail. We have elsewhere reported that apoSAA is bound to a subset of HDL particles containing apoA-I (12), following secretion of apoSAA monomer by hepatocytes (11). In this context, studies of the metabolism of apoSAA-rich HDL are appropriate for two reasons. Virtually nothing is known about the biologic properties of apoSAA-rich HDL during the acute-phase response. Also, the altered metabolism of apoSAA may be important in the formation of amyloid protein AA deposits during the pathogenesis of amyloidosis.

Results of trace labeling experiments clearly indicate that the metabolic behavior of both apoSAA isotypes is unique among HDL apoproteins to these polypeptides. For example, ~95% of the total  $^{125}\text{I}$ -apoSAA is cleared from the plasma by 6 h after intravenous administration of  $^{125}\text{I}$ -apoSAA-rich HDL, giving a provisional half-life estimate of ~85 min, as compared with 11 h for apoA-I. We note that this is an approximation from a limited number of data points and that factors contributing to initial clearance rates include the rapid turnover of denatured species and pool mixing with extravascular compartments. It is pertinent in this context that our estimate of  $^{125}\text{I}$ -apoA-I clearance rate in the mouse is similar to that reported for rat HDL and apoA-I (21, 22).

Compelling evidence that rapid apoSAA clearance is a property of the native molecule (rather than experimental artifact) was obtained in experiments in which to normal mice were administered fresh apoSAA-rich plasma and clearance of the administered dose was monitored by RIA. The clearance kinetics of the administered apoSAA was monoexponential through 3 h, with a plasma half-life of 72 min, a value comparable to that obtained in trace-labeling experiments with  $^{125}\text{I}$ -apoSAA-rich HDL.

One possible route of rapid  $^{125}\text{I}$ -apoSAA clearance, via urinary excretion of the apolipoprotein, was examined in trace-labeling experiments. No evidence for the selective urinary loss of apoSAA or apoSAA fragments was obtained. Furthermore, we find no evidence for the selective loss of apoSAA from the HDL particle *in vitro*, during repeated or prolonged ultracentrifugal fractionation of mouse apoSAA-rich HDL (unpublished observations).

In light of these results, we obtained a surprising finding in experiments originally designed to deter-

mine sites of apoSAA uptake. In these experiments (unlabeled) HDL was reconstituted with purified  $^{125}\text{I}$ -apoSAA, an approach that has been successfully used to study metabolism of other apolipoproteins (23, 24). In contrast to that observed in the experiments described above, the clearance kinetics of purified, reconstituted  $^{125}\text{I}$ -apoSAA paralleled that of similarly prepared  $^{125}\text{I}$ -apoA-I, i.e., rapid plasma  $^{125}\text{I}$ -apoSAA clearance was not observed. These results indicate that the property of rapid  $^{125}\text{I}$ -apoSAA clearance is not retained upon purification and reconstitution of this polypeptide with HDL.

Several possible explanations can be offered for the unique clearance behavior of apoSAA observed in the experiments described above. Clearance of apoSAA is perhaps specified by a structural domain(s) within the polypeptide that is labile to denaturing conditions used in the purification of  $^{125}\text{I}$ -apoSAA. Alternatively, apoSAA clearance may be specified by a subset of lipoprotein particles to which apoSAA is bound in native but not reconstituted form. A third alternative, that rapid clearance is specified by the selective, transient association of apoSAA with a fast-clearing non-HDL lipoprotein fraction is also possible. We cannot decide between these possibilities on the basis of present information.

Another approach to comparing the metabolic fate of apoSAA and other HDL apoproteins was to examine the tissue distribution of  $^{125}\text{I}$  at various time intervals following the administration of  $^{125}\text{I}$ -apoSAA-rich HDL, since the percent contribution of  $^{125}\text{I}$ -apoSAA to the total cleared  $^{125}\text{I}$ -protein varied with time. This approach was based upon the assumption that tissue measurements of radioactivity were not cumulative but reflected the quantity  $^{125}\text{I}$ -protein uptake at or near sampling times. For example, ~9, 6, and 2% of the administered  $^{125}\text{I}$ -apoSAA-rich HDL was localized in the major organs studied at 1, 6, and 24 h, respectively. The estimated percentage of total cleared  $^{125}\text{I}$ -apoprotein cleared as  $^{125}\text{I}$ -apoSAA ranged from ~50% (during the 1st h) to negligible (at 24 h). Examination of the tissue content of  $^{125}\text{I}$  at 1, 6, and 24 h postinjection indicates a similar distribution of radioactivity among the major organs examined at these times. Thus, we were unable to obtain evidence that the metabolic fate of  $^{125}\text{I}$ -apoSAA is different from that of other HDL apoproteins. A better understanding of the metabolic fate of  $^{125}\text{I}$ -apoSAA awaits the availability of a more suitable radiolabeled HDL preparation for such studies, e.g., one specifically labeled in the fast-clearing (undenatured) apoSAA moiety.

The association of apoSAA with the HDL has been confirmed in human (1), mouse (2), and rabbit plasma (3) (similar monkey HDL apoproteins have been reported [25]). The lipid-binding characteristics of

apoSAA were originally predicted from studies indicating that the human apoSAA NH<sub>2</sub>-terminal homologue, amyloid protein AA, contains two domains capable of forming amphipathic  $\alpha$ -helical segments (26). It remains to be determined whether rapid apoSAA clearance is a property common to species other than the mouse and whether this metabolic behavior is specified by a particular structural domain within the molecule.

The induction of hepatic apoSAA synthesis (6, 7, 27) by a macrophage-derived factor (7, 8) in response to bacterial endotoxin, the specific association of apoSAA with the HDL (1, 2, 11, 12), and the rapid plasma clearance of apoSAA reported here, implicate the involvement of apoSAA and apoSAA-rich HDL in an as yet undefined role in the acute-phase response. Interesting in this context are reports that bacterial endotoxins bind specifically to the HDL in vitro (28) and in vivo (29). Ulevitch et al. (28) showed that an alteration of certain physical and biologic properties of endotoxin occurred as the result of this interaction. This leads one to consider the possibility that apoSAA is involved in a response to endotoxin at the HDL particle surface. Apolipoproteins are known to function as cofactors in enzymatic processes, as signals for specific binding to cell surface receptors, and as determinants of lipoprotein particle structure (30). Further studies are required to determine the involvement of apoSAA in one or more of these capacities.

The massive extracellular deposits of amyloid protein AA fibrils that accumulate in various tissues during the progression of amyloidosis are generally thought to arise as the result of altered apoSAA metabolism. It is interesting, in this context, that spleen and kidney, major organs of amyloid protein AA deposition do not appear to be principally involved in the uptake of <sup>125</sup>I-apoSAA-rich HDL, as evidenced here. Our present findings emphasize the need for a detailed examination of apoSAA metabolism during the progression of amyloidosis and indicate that measurements of apoSAA concentration may inadequately reflect the rate of apoSAA production when compared with the plasma content of proteins having considerably longer half-lives in the circulation.

#### ACKNOWLEDGMENTS

We wish to thank Marlene Wambach for excellent technical assistance and Virginia Wejak for preparation of the manuscript.

This work was supported in part, by U.S. Public Health Service grant HL-03174. Dr. Hoffman was supported by U.S. Public Health Service cardiopathology training grant HL-07312.

#### REFERENCES

1. Benditt, E. P., and N. Eriksen. 1977. Amyloid protein SAA is associated with high density lipoprotein from human serum. *Proc. Natl. Acad. Sci. USA*. **74**: 4025-4028.
2. Benditt, E. P., N. Eriksen, and R. H. Hanson. 1979. Amyloid protein SAA is an apoprotein of mouse plasma high density lipoprotein. *Proc. Natl. Acad. Sci. USA*. **76**: 4092-4096.
3. Skogen, B., A. L. Børresen, J. B. Natvig, K. Berg, and T. E. Michaelsen. 1979. High-density lipoprotein as carrier for amyloid-related protein SAA in rabbit serum. *Scand. J. Immunol.* **10**: 39-45.
4. Anders, R. F., J. B. Natvig, T. E. Michaelsen, and G. Husby. 1975. Isolation and characterization of amyloid-related serum protein SAA as a low molecular weight protein. *Scand. J. Immunol.* **4**: 397-401.
5. Rosenthal, C. J., and E. C. Franklin. 1975. Variation with age and disease of an amyloid A protein-related serum component. *J. Clin. Invest.* **55**: 746-753.
6. Benson, M. D., and E. Kleiner. 1980. Synthesis and secretion of serum amyloid protein A (SAA) by hepatocytes in mice treated with casein. *J. Immunol.* **124**: 495-499.
7. Selinger, M. J., K. P. W. J. McAdam, M. M. Kaplan, J. D. Sipe, S. N. Vogel, and D. L. Rosenstreich. 1980. Monokine-induced synthesis of serum amyloid A protein by hepatocytes. *Nature (Lond.)*. **285**: 498-500.
8. Sztein, M. B., S. M. Vogel, J. D. Sipe, P. A. Murphy, S. B. Mizel, J. J. Oppenheim, and D. L. Rosenstreich. 1981. The role of macrophages in the acute-phase response: SAA inducer is closely related to lymphocyte-activating factor and endogenous pyrogen. *Cell. Immunol.* **63**: 164-176.
9. Benditt, E. P., and N. Eriksen. 1972. Chemical similarity among amyloid substances associated with long standing inflammation. *Lab. Invest.* **26**: 615-625.
10. Benditt, E. P., N. Eriksen, M. A. Hermanson, and L. H. Ericsson. 1971. The major proteins of human and monkey amyloid substance: common properties including unusual N-terminal amino acid sequences. *FEBS (Fed. Eur. Biochem. Soc.) Lett.* **19**: 169-173.
11. Hoffman, J. S., and E. P. Benditt. 1982. Secretion of serum amyloid protein and assembly of serum amyloid protein-rich high density lipoprotein in primary mouse hepatocyte culture. *J. Biol. Chem.* **257**: 10518-10522.
12. Hoffman, J. S., and E. P. Benditt. 1982. Changes in high density lipoprotein content following endotoxin administration in the mouse: formation of serum amyloid protein-rich subfractions. *J. Biol. Chem.* **257**: 10510-10517.
13. Anders, R. F., J. B. Natvig, K. Sletten, G. Husby, and K. Nordstoga. 1977. Amyloid-related serum protein SAA from three animal species: comparison with human SAA. *J. Immunol.* **118**: 229-234.
14. Schacterle, G. R., and R. L. Pollack. 1973. A simplified method for the quantitative assay of small amounts of protein in biological material. *Anal. Biochem.* **51**: 654-655.
15. McFarlane, A. S. 1958. Efficient trace-labelling of proteins with iodine. *Nature (Lond.)*. **182**: 53.
16. Bilheimer, D. W., S. Eisenberg, and R. I. Levy. 1972. The metabolism of very low density lipoprotein proteins. I. Preliminary *in vitro* and *in vivo* observations. *Biochim. Biophys. Acta*. **260**: 212-221.
17. Scanu, A. M., and C. Edelstein. 1971. Solubility in aqueous solutions of ethanol of the small molecular



- weight peptides of serum very low density and high density lipoproteins. *Anal. Biochem.* **44**: 576-588.
18. Goldsmith, M. R., E. C. Rattner, M. M. D. Koehler, S. R. Balikov, and S. C. Bock. 1979. Two-dimensional electrophoresis of small-molecular-weight proteins. *Anal. Biochem.* **99**: 33-40.
  19. Laemmli, U. K. 1970. Cleavage of structural proteins during the assembly of the head of the bacteriophage T4. *Nature (Lond.)*. **227**: 680-685.
  20. Gidez, L. I., J. B. Swaney, and S. Murnane. 1977. Analysis of rat serum apolipoproteins by isoelectric focussing. I. Studies on middle molecular-weight subunits. *J. Lipid Res.* **18**: 59-68.
  21. Roheim, P. S., D. Rachmilewitz, O. Stein, and Y. Stein. 1971. Metabolism of iodinated high density lipoproteins in the rat. I. Half-life in the circulation and uptake by organs. *Biochim. Biophys. Acta.* **248**: 315-329.
  22. Eisenberg, S., H. G. Windmueller, and R. I. Levy. 1973. Metabolic fate of rat and human lipoprotein apoproteins in the rat. *J. Lipid Res.* **14**: 446-458.
  23. Shepherd, J., C. J. Packard, A. M. Gotto, Jr., and O. D. Taunton. 1978. Comparison of two methods to investigate the metabolism of human apolipoprotein A-I and apolipoprotein A-II. *J. Lipid Res.* **19**: 656-661.
  24. van't Hooft, F., and R. J. Havel. 1981. Metabolism of chromatographically separated rat serum lipoproteins specifically labeled with <sup>125</sup>I-apolipoprotein E. *J. Biol. Chem.* **256**: 3963-3968.
  25. Parks, J. S., and L. L. Rudel. 1979. Isolation and characterization of high density lipoprotein apoproteins in the non-human primate (Vervet). *J. Biol. Chem.* **254**: 6716-6723.
  26. Segrest, J. P., and R. J. Feldmann. 1977. Amphipathic helices and plasma lipoproteins: a computer study. *Biopolymers.* **16**: 2053-2065.
  27. Morrow, J. F., R. S. Stearman, C. G. Peltzman, and D. A. Potter. 1981. Induction of hepatic synthesis of serum amyloid A protein and actin. *Proc. Natl. Acad. Sci. USA.* **78**: 4718-4722.
  28. Ulevitch, R. J., A. R. Johnston, and D. B. Weinstein. 1979. New function for high density lipoproteins. Their participation in intravascular reactions of bacterial lipopolysaccharides. *J. Clin. Invest.* **64**: 1516-1524.
  29. Freudenberg, M. A., T. C. Bøg-Hansen, U. Back, and C. Galanos. 1980. Interaction of lipopolysaccharides with plasma high density lipoprotein in rats. *Infect. Immun.* **28**: 373-380.
  30. Osborne, J. C., and H. B. Brewer. 1978. The plasma lipoproteins. *Adv. Protein Chem.* **31**: 253-337.